applied sciences

MDPI

Article

Effect of Vascular Lumen Reduction on the Performance and Energy Consumption of an Innovative Implantable LVAD

Ryszard Jasinski [1,2], Krzysztof Tesch [1,2,*], Leszek Dabrowski [1,2] and Jan Rogowski [2,3]

[1] Faculty of Mechanical Engineering and Ship Technology, Gdansk University of Technology, 80-233 Gdansk, Poland; ryszard.jasinski@pg.edu.pl (R.J.); ldabrows@pg.edu.pl (L.D.)
[2] Medarch Ltd., ul. Piaskowa 3, 83-110 Tczew, Poland; janrog@gumed.edu.pl
[3] Department of Cardiac and Vascular Surgery, Medical University of Gdansk, 80-210 Gdansk, Poland
* Correspondence: krzyte@pg.edu.pl

Abstract: This paper presents the results of a study on the effect of vascular lumen reduction on the performance of an innovative implantable LVAD (left ventricular assist device). It details the pressures in the individual cardiac chambers as a function of device frequency. In addition, mass flow rates and energy consumption of the device are examined, varying with lumen reduction and operating frequency. While the lumen reduction of the vessels has little effect on energy consumption, the mass flow rates vary considerably, i.e., above 140 cyc/min, the mass flow rate increment is no longer achieved for specified initial conditions. There are also differences regarding the pressures in the heart; namely, it was found that the pressure plots look similar in all cases, leading to the conclusion that the reduction of the vessel lumen does not affect their shape, but does affect the maximum values of the left ventricular and aortic pressures. Importantly, the innovative device in the form of an intra-cardiac balloon assembly for circulatory support is based on a pulsatile flow strategy and is synchronized with the ECG signal. Other advantages of the proposed solution include a minimally invasive method of implantation, which is important for patients with end-stage heart failure. The design of the device is portable and the device itself is battery-powered, allowing for shorter hospitalization times and faster recovery, even in patients with end-stage heart failure associated with mitral regurgitation and pulmonary hypertension.

Keywords: heart-assist devices; implantable assist device; left ventricle; intra-cardiac balloons

Citation: Jasinski, R.; Tesch, K.; Dabrowski, L.; Rogowski, J. Effect of Vascular Lumen Reduction on the Performance and Energy Consumption of an Innovative Implantable LVAD. *Appl. Sci.* **2024**, *14*, 284. https://doi.org/10.3390/app14010284

Academic Editor: Zhonghua Sun

Received: 30 October 2023
Revised: 25 December 2023
Accepted: 26 December 2023
Published: 28 December 2023

1. Introduction

According to the WHO, cardiovascular diseases are the leading causes of death globally, estimated to claim 17.9 million lives each year [1]. Furthermore, heart failures caused by a reduced or impaired blood pumping function of the heart, affect 64.3 million patients annually [2]; this includes pediatric patients [3] and is associated with high morbidity and mortality. Unfortunately, despite ongoing developments in cardiac surgery, it is also estimated that more than 40% of patients diagnosed with heart failure will die within five years [4–6]. The same applies to pharmacological treatment, which can only slow down the process. The standard and best solution for patients with advanced heart failure is heart transplantation [7]. Transplantation is not always possible due to the shortage of donors [8], long waiting lists [9], high costs [10], problems with organ rejection, and high mortality [11].

Left ventricular assist devices (LVADs) are typically used as a bridge to heart transplant [12], as a bridge to recovery, or as destination therapy [13]. The former is used when medical treatment (conservative treatment) or surgery (e.g., heart transplantation) are no longer options, or are simply unsuccessful at preventing further deterioration. A bridge to recovery is cardiac support intended for use while the heart recovers, at a time when it is too weak. Finally, destination therapy is for patients who do not qualify for a heart

transplant. This also means that destination therapy provides permanent cardiac support. Moreover, LVADs are used for both short-term therapy and destination therapy, and they are considered an effective therapeutic approach as a bridge to heart transplantation [14].

LVADs in the form of mechanical pumps consist of several components, including inflow and outflow cannulae, the pump itself, a battery pack, and a controller. Some of these components are implantable. The most important component is the mechanical pump, which replaces or supports the action of the failing heart and is controlled by a controller. The most commonly implantable parts are cannulae, the shape of which is also subject to optimization [15]. The most well-known and popular intra-aortic pumps include Impella®, POLVAD [16], Levitronix CentriMag™, TandemHeart™, HeartMate 3™, HeartWare™, MicroMed DeBakey [17], and EXCOR® Berlin Heart. Moreover, the intra-aortic balloon pumps and VA ECMO (veno-arterial extracorporeal membrane oxygenation) [18,19] can also be added to the above. However, it is important to be aware of the potential complications associated with the use of certain devices, which may include bleeding, requiring transfusion, infection, hemolysis, and limb ischemia [20]. The second major limitation is that the aforementioned devices are mostly designed for temporary support during hospitalization. The exceptions may, however, be HeartMate 3™ and HeartWare™, only if continuous monitoring is possible.

Total artificial hearts and ventricular assist devices have been developed for decades [21]. While the former aim to completely replace the function of the heart, the latter merely assist the function of the failing heart by supporting it. The first generation of pumps were pulsatile flow pumps, which were the dominant solution until 2009 [22]. Interestingly, pulsatile flow pumps mimic the cyclic action of the heart using artificial heart valves, which consequently contributes to their large size and weight. The noise generated by this type of equipment was also not insignificant. Since 2010, the next generation of pumps, namely continuous flow pumps, has been in widespread and almost exclusive use [23,24]. The biggest advantages of continuous flow pumps include their smaller size and reduced noise generation. Another significant advantage is their portability, allowing patients greater freedom of movement. Continuous flow pumps are further categorized into axial and centrifugal pumps. While axial pumps are smaller in size, they require considerably higher rotational speeds compared to centrifugal pumps [25], which may lead to thrombosis [5,26] and hemolysis [27,28]. However, by optimizing the shape of the axial pump, the necessary rotational speed can be reduced for the same pressure increase [29]. Constant pressure is also a feature of this type of pump, which can further lead to cardiac arrhythmia [30]. The design of the impellers in centrifugal pumps allows for a significant reduction in their rotational speeds, which are two to three times lower than those of axial pumps. This speed comes at the expense of larger impeller diameters.

New solutions are being proposed all the time. An example is a total artificial heart operating on the principle of valveless pumping, featuring a rotating and linearly shuttling piston within a cylindrical housing [31]. Another example would be a continuous-flow total artificial heart that operates without valves and is suspended both axially and radially through the balancing of the magnetic and hydrodynamic forces to improve biocompatibility [32]. Yet another example is a low-cost device for long-term use containing a rim-driven, hubless, axial flow pump, as well as the wireless transmission of energy [25].

Since most of the available designs require highly invasive medical procedures, there is still a need for a new left ventricular assist device whose implantation will not significantly burden patients. This applies, in particular, to patients with end-stage heart failure. The device proposed in this study (first introduced in [33,34]) requires minimally invasive implantation and, thus, significantly reduces hospitalization time, which is highly significant for patients with end-stage heart failure, along with mitral regurgitation and pulmonary hypertension.

This paper extends the research presented in [35] by investigating the effect of reduced lumen on the performance of an innovative left ventricular support device. The reduction of the vascular lumen was achieved by changing the cross-sectional area of the adjustable

hydraulic valve, which is located a short distance from the aorta. It can be assumed that this configuration mimics the effect of aortic stenosis. Investigating the effect of reducing the vessel lumen allows us to study the behavior of the device under unfavorable conditions, which are associated with an increase in flow resistance, which can further lead to increases in pressure in the heart chambers and balloons. This is very important for the safety of the device and, above all, the patient. Moreover, the performance of the device at very high operating frequencies (of up to 160 cyc/min) is investigated. Additional results show the impact of energy consumption as a function of the operating frequency and the mass flow rates generated by the device, which are related to the ability to provide the required flows. Importantly, the innovative device is based on a pulsatile flow strategy and is synchronized with the heart cycle.

2. Principle of Operation of the Innovative Device

A CAD model of the left ventricle with limited myocardial contractility is presented in Figure 1. A description of the procedure for reconstructing the heart geometry from selected computed tomography angiography is presented in [35]. In brief, the model considered the left ventricle, atrium, and aorta for a left ventricular ejection fraction of 30% in both systole and diastole, which corresponds to a case with chronically low ejection fraction. The geometry was derived from a patient with mitral valve regurgitation and a certain degree of chronic post-myocardial infarction heart failure.

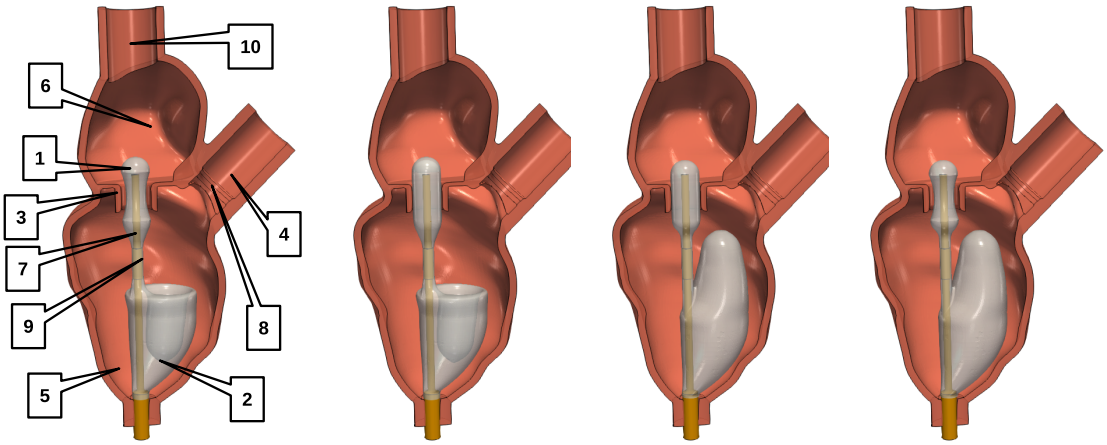

Figure 1. Principle of operation: (1)—valve balloon; (2)—ventricular balloon; (3)—cylindrical orifice (mitral valve); (4)—aorta; (5)—left ventricle; (6)—left atrium; (7)—pneumatic line; (8)—aortic valve location; (9)—narrowing; (10)—single conduit to the atrium. (**a**) start of diastole. (**b**) end of diastole. (**c**) start of systole; (**d**) end of systole.

As the device is transcatheter implantable, which does not require extensive surgical intervention, it only takes its final shape in the left ventricle when the balloons take their final shapes and volumes. The shape of these balloons is specifically chosen to correspond to the anatomical shape of the left ventricle.

The principle of operation and a schematic diagram of the device, which is located in the left ventricle in its unfolded state, are shown in Figure 1. There are four characteristic stages, i.e., the start and end of cardiac systole and diastole, which correspond to the respective inflation or deflation of the individual balloons of the device. In the condition in Figure 1a, which is defined as the start of diastole, the ventricular (2) and valve balloons (1) are deflated. Both balloons are flexible and connected by a narrowing (9). The ventricular balloon is considerably larger than the valve balloon, which is positioned in the mitral valve area (3). In the heart model, the regurgitant mitral valve is represented by a circular orifice (3). At the beginning of diastole in Figure 1a, the aortic valve is closed. Moreover, the heart model includes an artificial mechanical aortic valve located at position (8). With

the mitral valve open, blood flows through the conduit (10) into the atrium (6) and then into the left ventricle (5) via the cylindrical orifice (3). In this model, the conduit (10) serves as a replacement for the pulmonary arteries.

The next characteristic state is the end of diastole, which is shown in Figure 1b. Namely, the mitral valve (3) is occluded with a valve balloon (1), which stops the inflow of blood from the atrium (6). Then, the end of diastole is followed by the beginning of systole, which is shown in Figure 1c. It can be observed that the ventricular balloon (2) is inflated while the valve balloon (1) is simultaneously inflated, leading to an increase in ventricular pressure and the opening of the aortic valve (8). This results in the ejection of blood into the aorta (4), marking the transition to the last stage—end of systole—as shown in Figure 1d. In this last stage, the valve balloon (1) is closed and the mitral valve (3) is open, followed by the beginning of the deflation of the ventricular balloon (2).

What is extremely important is that the functioning of the device is based on a pulsatile flow strategy, which is implemented by means of cyclic inflation and deflation of the balloons synchronized to the heart cycle. Control signals are transmitted to the device via the ODROID computer, which analyzes the ECG signal, based on which, it initiates the inflation and deflation of individual balloons. The balloons are supplied via a pneumatic line (7). In this case, a single line was used for both inflating and deflating. Adequate synchronization was achieved by correctly locating a certain number of orifices/outlets in the pneumatic line, as well as selecting appropriate diameters. Some of the orifices are located within the valve balloon and the rest within the ventricular balloon. Finally, the gas (helium) is supplied through a pneumatic line (7) by means of an external gas supply system (described in the next paragraph), of which, the suction–discharge device is a part of.

3. Methods—Experimental Stand

In order to study the effect of reduced lumen in blood vessels on the performance of the left ventricular assist device, the experimental setup shown in Figure 2 was constructed. This stand is equipped with a flexible heart model containing a set of balloons, i.e., a ventricular balloon and a valve balloon. The ventricular balloon is used in order to pump fluid (artificial blood) from the left ventricle into the circulatory system, while the valve balloon ensures the occluding of the valve orifice (regurgitant valve opening). To ensure that the operating conditions of the circulatory system closely resemble real-life conditions, the hydraulic system was enhanced with compensation vessels. These vessels simulate the flexibility of the human circulatory system. Additionally, an adjustable hydraulic valve was incorporated to alter the flow resistance within the hydraulic system. A mechanical aortic valve (check valve) was placed in the fluid flow line. In addition, a flexible transparent heart model was printed from resin on a 3D printer. Through the transparent wall of the model, the operation of the ventricular and valve balloons could be observed.

More than a dozen sensors were placed in the hydraulic (artificial blood) and pneumatic systems (helium). Pressure sensors (High Precision Transmitter ATM.1ST STS Sensor Technik Sirnach) allowed pressure to be measured at several locations in the hydraulic system, even in the left ventricle and atrium of the heart model. The aortic pressure sensor was located at the beginning of the aorta (behind the aortic valve) rather than downstream of the valve, as this made it possible to compare the pressure in the aorta with the pressure in the left chamber. Also, the so-called Wiggers diagrams (described in the next paragraph) show pressure plots in this part of the aorta. The pressure of the gas in the pneumatic system close to the balloon assembly was measured using the SPAU-B2R-H sensor from Festo. Moreover, the flow rate in the hydraulic system was also determined using a highly accurate Optibatch 4011 C from Krohne. An electric heater was also placed in the hydraulic system to maintain the temperature of the fluid at around 34–36 °C. In addition, data, such as liquid temperature and liquid density, were read from the artificial blood flow rate measuring device.

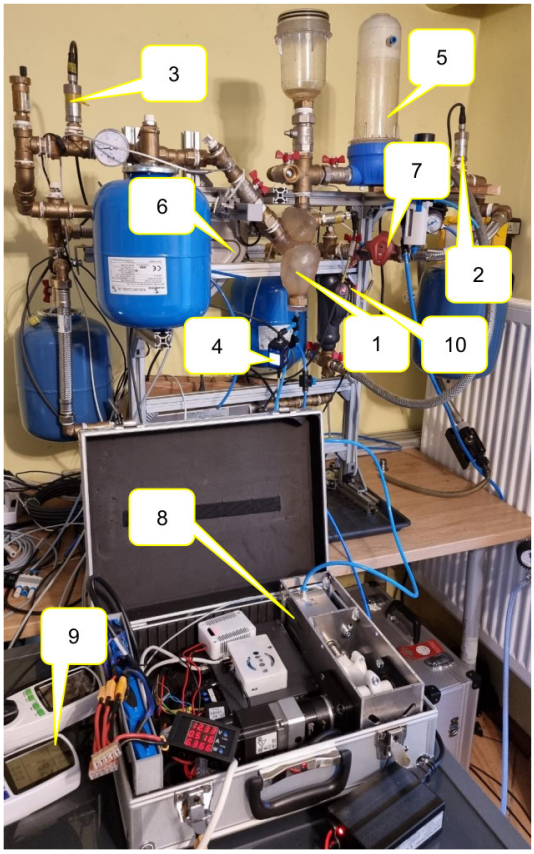

Figure 2. Experimental stand: (1)—flexible left heart; (2)—pulmonary veins pressure sensor; (3)—aorta pressure sensor; (4)—gas (helium) pressure sensor near balloons; (5)—flow reservoir replacing the pulmonary veins; (6)—flow meter; (7)—hydraulic valve for changing reduction of the blood vessel lumen; (8)—external helium supply system; (9)—system for measuring the power consumption of the external helium supply system; (10)—electric heater.

Measurements of the circulatory system were taken, i.e., pressure in front of and behind the heart model ((2), (3) in Figure 2), pressure in the atrium and left ventricle of the heart model, and the flow rate (flow meter (6) in Figure 2). Gas pressure was measured in the pneumatic system in front of a set of balloons placed in the heart model ((4) in Figure 2). The testing of the left ventricular assist device was performed at balloon set operating frequencies of 60, 100, 120, 140, and 160 cyc/min.

The designed and constructed stand (Figure 2) enables the modeling of the impact of reduced blood vessel lumen on the performance of the LVAD. In this stand, a very important role is played by the control valve (7) in Figure 2, which facilitates the regulation and variation of the flow resistance in the hydraulic (blood) system. Using this valve, three different loads on the hydraulic system were obtained, which correspond to the reduced lumen of the blood vessels, namely

- Case 0—No reduction in the blood vessel lumen, i.e., fully open valve (7) in Figure 2;
- Case 1—The first stage of reducing the blood vessel lumen. This involves partially closing the adjustable valve (7), thereby reducing the flow cross-sectional area. The valve is gradually closed until there is a noticeable change in the flow rate;
- Case 2—The second stage of reducing the blood vessel lumen. This is achieved by further partial closure of the adjustable valve (7), reducing the flow cross-sectional area more significantly. The valve is closed to the point where a reduction in the flow rate becomes visible.

The reduction of the vessel lumen was achieved by altering the cross-sectional area of an adjustable hydraulic valve. This valve is designed to increase the resistance to fluid flow

in the hydraulic system installation, a direct consequence of changes in its cross-sectional area. Moreover, the vessel lumen reduction valve is located in the center of the hydraulic system of the test stand. It can be assumed that this valve is positioned a short distance from the aorta, considering the compact arrangement of the hydraulic system's components and the unobstructed flow within it. Adjusting the valve setting significantly impacted the system's response to the tested parameters of both the external (suction–discharge device) and internal (balloon set) systems in operation.

Furthermore, a metering system was built to determine the power consumption of the two systems:

- A system with the Mitsubishi servo amplifier powering the Mitsubishi servo motor ((1) in Figure 3) where the system was powered directly from the 230 V AC. The power consumed by this system will be designated P_2;
- A system with a 12 V DC to 24 V DC converter ((5) in Figure 3) and a sensor for determining the position of the compressor system base point and a 12 V DC to 5 V DC converter ((6) in Figure 3) to power the ODROID computer ((4) in Figure 3). The system was powered from a 12 V DC battery pack ((3) in Figure 3). The power consumed by this system will be designated as P_1.

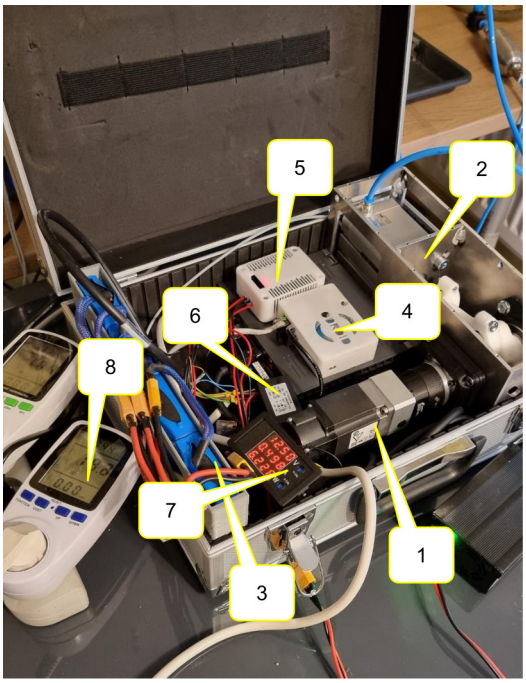

Figure 3. External gas supply system for the balloon system, consisting of a servo-driven reciprocating compressor with a crank mechanism and measuring system: (1)—servo motor: (2)—reciprocating compressor; (3)—battery pack; (4)—ODROID computer; (5)—12 V DC to 24V DC converter to power the piston position sensor in the actuator to base the compressor system; (6)—12 V DC to 5 V DC converter to provide 5 V voltage to power the ODROID computer; (7)—system measuring the energy consumption of the 12 V DC to 24 V DC converter to power the piston position sensor in the actuator to base the compressor system and 12 V DC to 5 V DC converter to provide 5 V voltage to power the ODROID computer; (8)—system measuring the energy consumption of the servo motor and servo amplifier.

The measurement of the power consumption was made directly on these systems of electrical components. This was a direct measurement of the energy consumption of all electrical components present in the balloon assembly's external gas supply system. If the external gas supply system does not use the 230 V AC to power the servo amplifier and servo motor directly, the power consumption will be even higher. The energy consumption

study omitted the voltage converter from 12 V DC to 230 V AC between the electric battery pack and the servo amplifier system powering the servo motor.

A very important part of the external gas supply system is the so-called suction–discharge device, which consists of the servo motor (1) and reciprocating compressor (2) in Figure 3. This device is designed to inflate and deflate balloons according to the cycle of the heart, which is controlled by an ODROID computer (4) in Figure 3. This computer processes the ECG signal in real time, further ensuring accurate control as required. In addition to the control functions, the ODROID computer allows control and monitoring of the most important parameters of both the heart and the device, which further translates into safety. Furthermore, in the suction–discharge device, the rotational motion of the servo motor is converted via the crank system into the reciprocating motion of the compressor piston. The compressor piston has a diameter of 50 mm. In the current study, a cranking system was used in the suction–discharge device to provide a 40 mm displacement (stroke) of the compressor piston (reciprocating movement). Moreover, the external gas supply system dimensions are as follows: width 400 mm, depth (length) 300 mm, height 135 mm. Weight of case without battery pack 6.11 kg, battery pack with printed basket (housing): 1.51 kg.

4. Results and Discussion

4.1. Pressure Measurements

Initially, the hydraulic system was filled with a preliminary liquid (mixture) with properties resembling human blood, which was a solution of water and glycerine. The glycerine was then slowly and gradually added to the hydraulic system. The liquid, meanwhile, was flowing in the hydraulic system due to the working external and internal systems. The Optibatch 4011 flow meter used had the ability to measure density. The temperature of the liquid was maintained via a flow-through electric heater. Once the correct density was achieved, the performance (parameters) of the external and internal systems began to be tested. The viscosity of a liquid (a mixture of glycerine and water) can be derived from its density and temperature. Also, since the Coriolis mass principle was used for the flow measurement, the viscosity and density parameters had no influence on the flow measurement. The density of the liquid was approximately 1060 kg m^{-3}. A vacuum was then created in the pneumatic system. After checking that the pneumatic system was airtight, it was filled with helium. The system was filled to an initial pressure of 75 mm Hg with the compressor piston of the portable balloon supply system retracted.

4.1.1. Case 0—No Reduction in the Blood Vessel Lumen

The fluid pressure plots in the ventricle and aorta were similar to one another during the inflation of the ventricular balloon, i.e., the pumping of fluid into the hydraulic system during the cardiac contraction cycle (systole). Also, the left ventricular pressure was slightly higher for this period compared to aortic pressure values (Figure 4a). Figure 4c shows the maximum fluid pressure values measured in the aorta (after the heart model), the left ventricle of the heart model, obtained during testing of the hydraulic system with the control valve open, meaning that there was no reduction in the blood vessel lumen. The maximum fluid pressures p_{max} in the aorta, depending on the frequency f of operation of the device between 60 and 160 cyc/min, ranged from 113 mm Hg for 60 cyc/min to 157 mm Hg for 140 cyc/min (Figure 4c). The differences in the maximum fluid pressures in the hydraulic system in the left heart ventricle and aorta were in the range of approximately 27 to 34 mm Hg, depending on the frequency of the device.

The pressure in the pneumatic system, as measured with a pressure sensor located near the balloon set for the external gas supply system operating frequencies of 60, 100, 120, 140, and 160 cyc/min, ranging from about −170 mm Hg to about 732 mm Hg (Figure 4b). The maximum gas (helium) pressures upstream of the balloon set, when the control valve in the hydraulic system was open, varied from 443 mm Hg for 60 cyc/min to about 732 mm Hg for 160 cyc/min (Figure 4c).

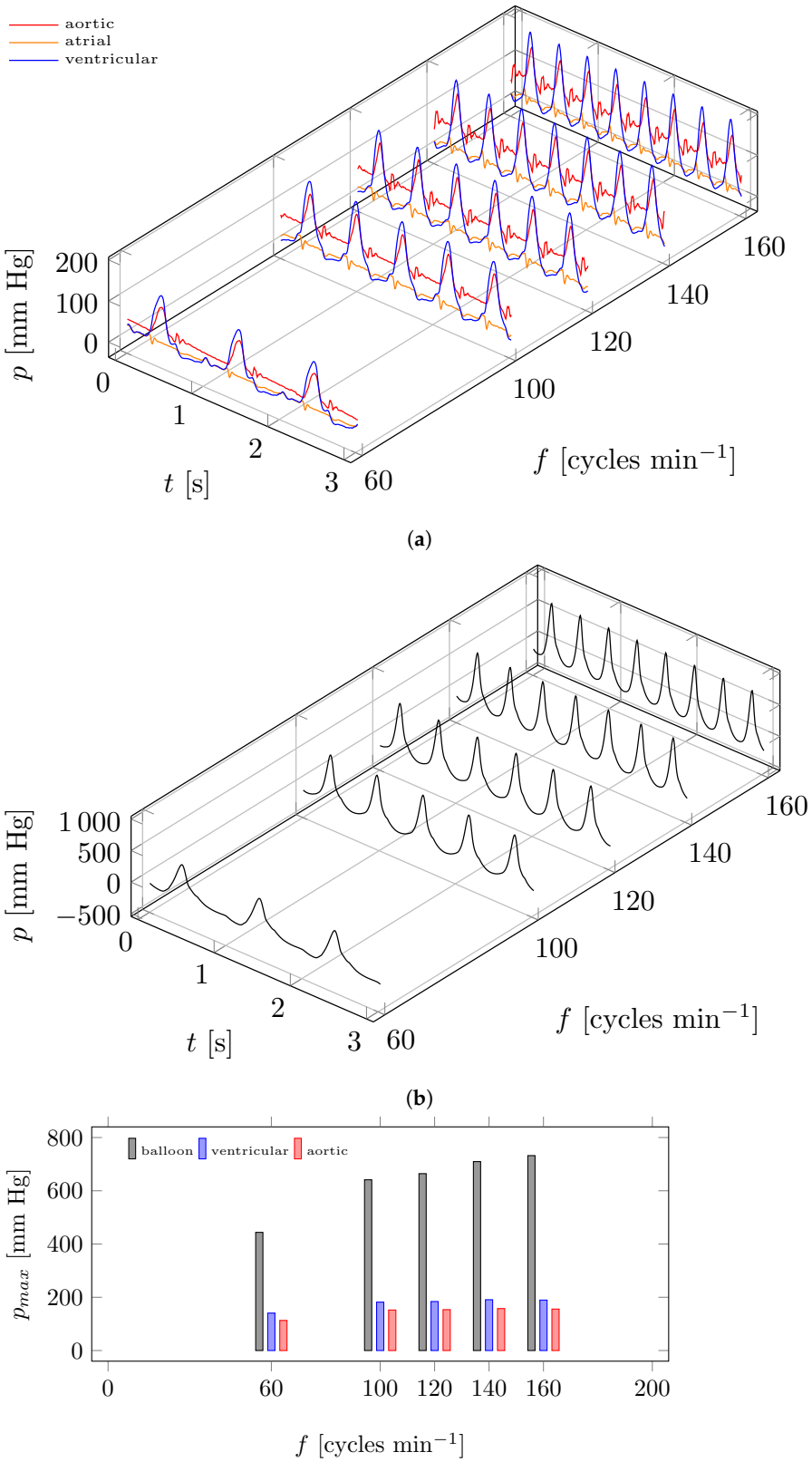

Figure 4. Pressures p in the hydraulic–pneumatic system for different operating frequencies f of the device for case 0—no reduction in the blood vessel lumen. (**a**) Fluid pressures in the hydraulic system as measured by the sensors. (**b**) Pressure p in the pneumatic system measured by a pressure sensor placed near the balloon assembly. (**c**) Maximum pressure values p_{max}.

4.1.2. Case 1—First Stage of the Reduction of the Blood Vessel Lumen

Figure 5a shows the fluid pressure values in the left ventricle and aorta. This time, the shapes of the measurements (red and blue colors) were also similar to each other during the inflation of the ventricular balloon, i.e., the pumping of fluid into the hydraulic system that corresponded to cardiac contraction. This means that there were no significant changes between the aortic and ventricular pressure waveforms during balloon inflation. The pressure values in the ventricle were slightly higher for this period compared to the pressure values in the aorta. The maximum fluid pressure p_{max} values, measured in the aorta and the left ventricle, are shown in Figure 5c. The measurements were obtained during the testing of the hydraulic system with the control valve partially closed (the first stage of the reduction of the blood vessel lumen). The maximum values of fluid pressure in the aorta, depending on the frequency f of operation of the device between 60 and 160 cyc/min, ranged from 124 mm Hg for 60 cyc/min to 168 mm Hg for 120 cyc/min. The differences in the maximum fluid pressures in the hydraulic system in the left ventricle and aorta, depending on the frequency f of operation of the device in the range of 60 to 160 cyc/min, were from approximately 27 to 37 mm Hg.

The pressure in the pneumatic system, as measured by a sensor located near the balloon set for the external gas supply system, varied across operating frequencies of 60, 100, 120, 140, and 160 cycles per minute. The pressure range was approximately from about −164 mm Hg to about 733 mm Hg (Figure 5b). The maximum gas (helium) pressure in front of the balloon set, varied from 464 mm Hg for 60 cyc/min to about 733 mm Hg for 160 cyc/min (Figure 5c).

4.1.3. Case 2—Second Stage of the Reduction of the Blood Vessel Lumen

Fluid pressures in the ventricle and aorta were similar to one another during ventricular balloon inflation, similar to the previous two cases. Again, the left ventricular pressure values were slightly higher for this period compared to the aortic pressure values (Figure 6a). Figure 6c shows the maximum values of fluid pressure p_{max} measured in the aorta and left ventricle, which were obtained during testing of the hydraulic system with an even more closed control valve (second stage of the reduction of the blood vessel lumen). Maximum aortic fluid pressures ranged from 152 mm Hg for 60 cyc/min to 187 mm Hg for 120 cyc/min, depending on the frequency f of operation of the device (Figure 6b). The differences in maximum fluid pressures within the hydraulic system, specifically in the heart ventricle and aorta, varied, depending on the operating frequency of the device, which ranged from 60 to 160 cyc/min. These differences were approximately between 26 and 37 mm Hg.

The pressure in the pneumatic system, measured with a pressure sensor located near the balloon set for the external gas supply system, exhibited operating frequencies of 60, 100, 120, 140, and 160 cyc/min, ranging from about −154 mm Hg to about 740 mm Hg (Figure 6b). The maximum gas (helium) pressure in front of the balloon set varied from 494 mm Hg for 60 cyc/min to about 740 mm Hg for 160 cyc/min (Figure 6c).

4.2. Measurement of Energy Consumption and Flow Rate

The results of the energy consumption (power consumed) obtained with the constructed measuring system are shown in Figure 7. Two configurations can be distinguished:

- Servo amplifier configuration powering a servo motor (supplied directly from the 230 V AC). The power of this configuration is designated as P_2;
- Configuration with a 12 V DC to 24 V DC converter and a sensor for determining the position of the compressor system base point and with a 12 V DC to 5 V DC converter to power the ODROID computer (powered by a set of 12 V DC batteries). The power of this configuration designated as P_1.

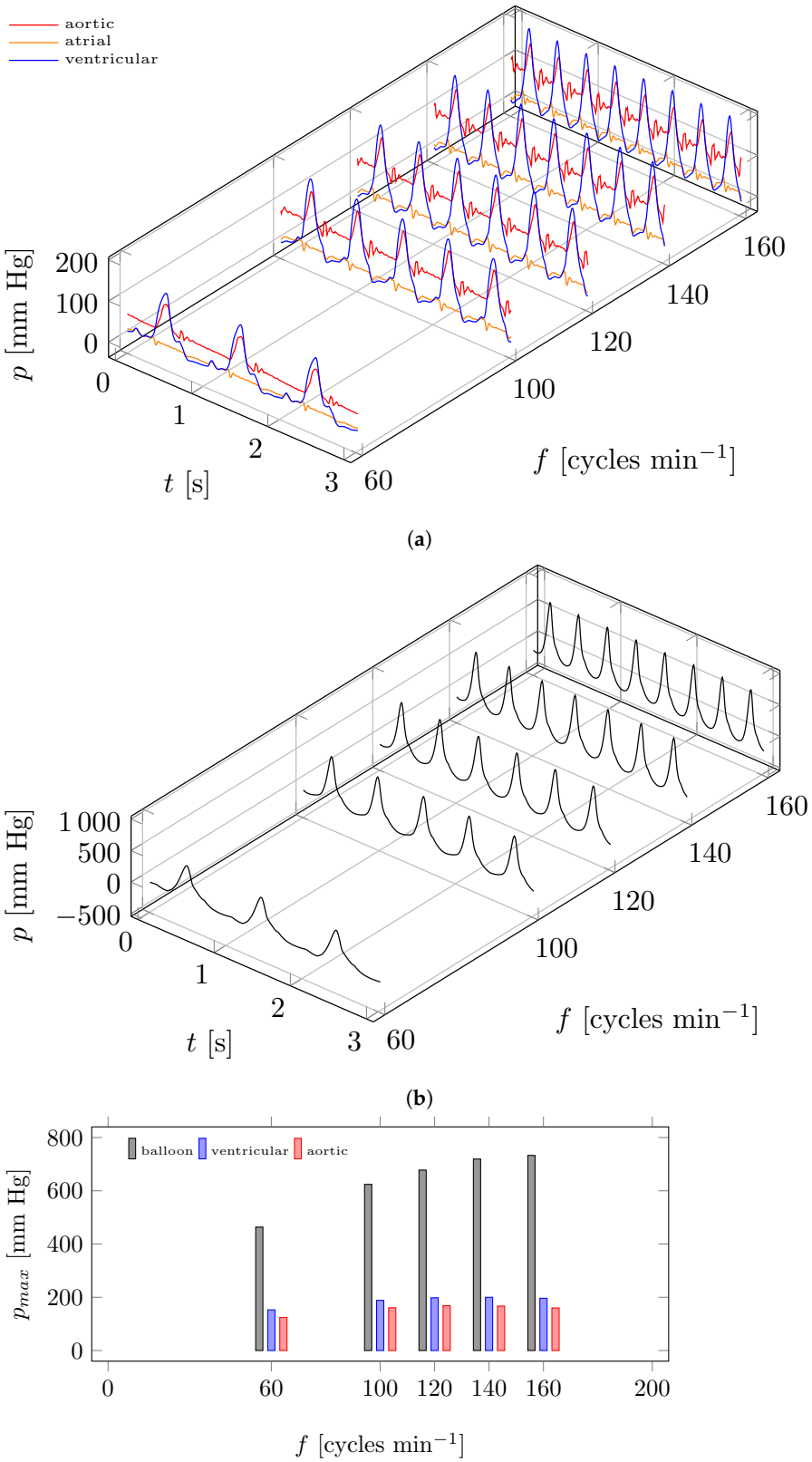

Figure 5. Pressures p in the hydraulic-pneumatic system for different operating frequencies f of the device for case 1—first stage of the reduction of the blood vessel lumen. (**a**) Fluid pressures in the hydraulic system as measured by the sensors. (**b**) Pressure p in the pneumatic system measured by a pressure sensor placed near the balloon assembly. (**c**) Maximum pressure values p_{max}.

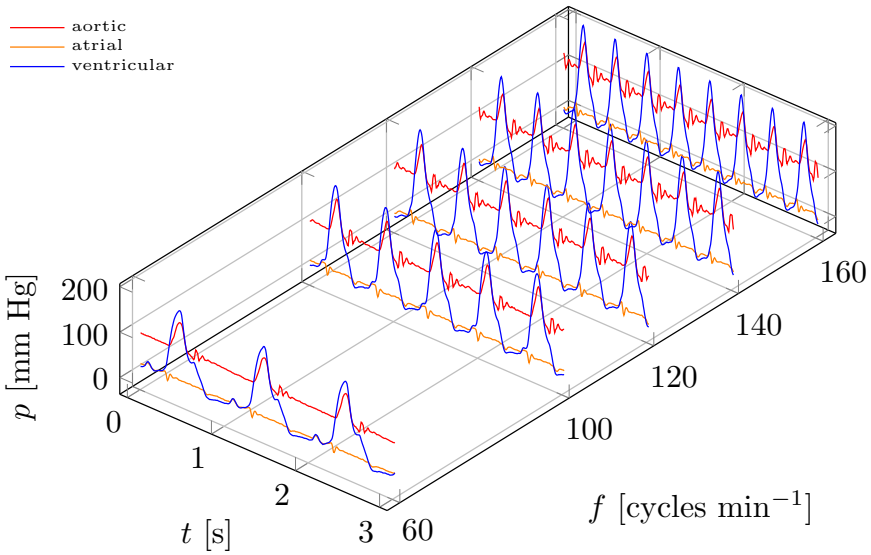

(**a**)

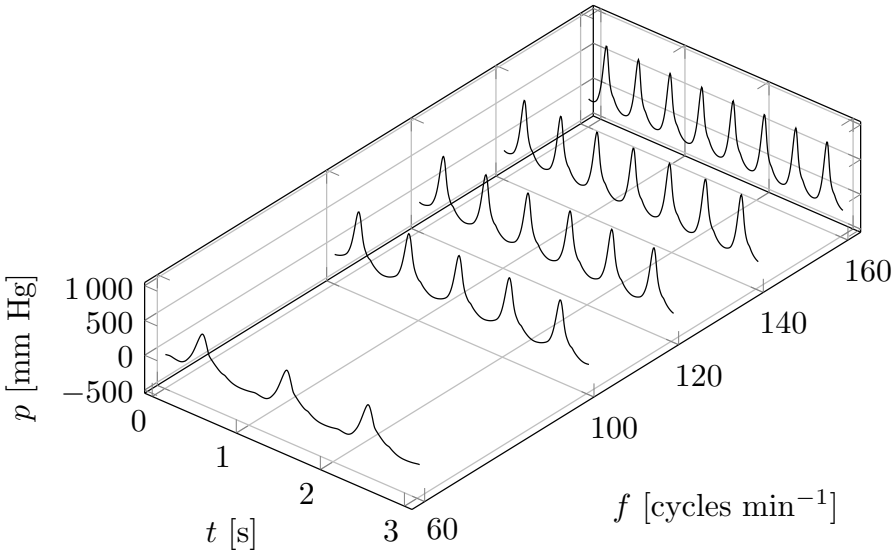

(**b**)

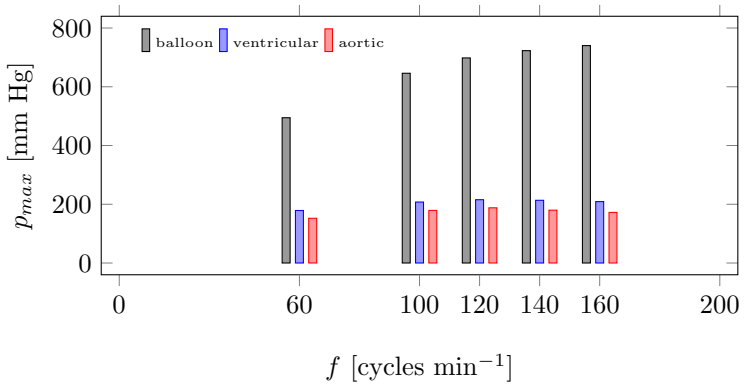

(**c**)

Figure 6. Pressures p in the hydraulic-pneumatic system for different operating frequencies f of the device for case 2—second stage of the reduction of the blood vessel lumen. (**a**) Fluid pressures in the hydraulic system as measured by the sensors. (**b**) Pressure p in the pneumatic system measured by a pressure sensor placed near the balloon assembly. (**c**) Maximum pressure values p_{max}.

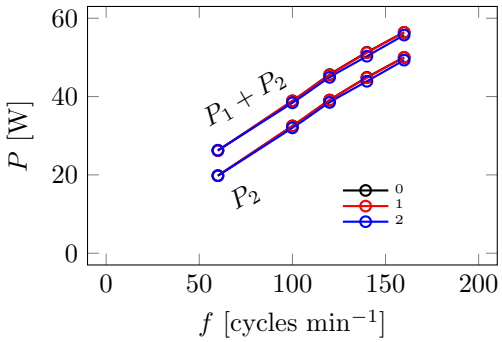

Figure 7. Power P consumed by the servo drive P_2 (a system with the servo amplifier and servo motor) and power consumed by two systems $P_1 + P_2$: servo drive P_2 plus the control system P_1 (system with 12 V DC to 24 V DC converter and a sensor for determining the position of the compressor system base point and 12 V DC to 5 V DC converter and ODROID computer); 0—no reduction-, 1—first-, 2—second stage of the reduction of the blood vessel lumen.

The power P_2 consumed by the servo amplifier system, which powers the servo motor, varies linearly with the frequency f of the balloons. More specifically, at a frequency of $f = 60$ cyc/min, P_2 varies from about 20 W to 50 W at a frequency of $f = 160$ cyc/min. The power requirements of this configuration can be approximated by a linear function of the following form:

$$P_2 = 2 + 0.3\,f \qquad \text{W} \tag{1}$$

where f is the frequency in cyc/min.

The power of the configuration with the 12 V DC to 24 V DC converter and the sensor for determining the compressor system base point position and the 12 V DC to 5 V DC converter feeding the ODROID computer P_1 is the same for all tests (around 6.4 W).

Reducing the lumen of the blood vessels (simulated by closing the control valve) significantly affects the value of the mass flow rate $\dot{m}$ (Figure 8). Very large differences in the mass flow rate $\dot{m}$ between cases occur at the maximum heart rate (160 cyc/min) compared to the minimum heart rate (60 cyc/min). It can be seen that the flow rate variation in the hydraulic system when controlling the valve from fully open (0—no reduction) to partially closed (1—first stage of reduction) is as high as approximately 0.5 kg/min. In contrast, the change in the mass flow rate during valve setting from partially closed (1—second stage of reduction) to even more closed (2—second stage of reduction) is as high as approximately 0.6 kg/min. Meanwhile, for a frequency of 60 cyc/min, the differences in mass flow rate for individual cases do not exceed 0.2 kg/min. It is also important to note that increasing the operating frequency above 140 cyc/min does not generally increase the mass flow rate, except in the case where there is no reduction of the vessel lumen. In all cases, the greatest changes occur in the frequency range of 60 to 100 cyc/min. Increasing the frequency from 60 to 160 cyc/min increases the flow rate by 50% in the case of no reduction of the lumen of the vessels. In the case of lumen reduction, the values are smaller.

4.3. Discussion

In general, it can be observed that the pressure plots appear qualitatively similar across all cases. Thus, while the reduction of the blood vessel lumen does not affect the shape of these plots, it does influence their maximum values. The smallest changes in the maximum pressures, p_{max}, in the left ventricle and aorta occur between case 0 (no reduction in blood vessel lumen) and case 1 (first stage of reduction). These pressures increase in case 2 (second stage of reduction). Increasing the operating frequency, on the other hand, increases the balloon pressure for all vessel lumen reduction values.

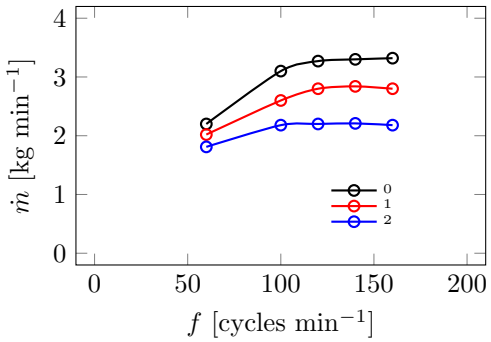

Figure 8. Mass flow rate $\dot{m}$ for different operating frequencies f as a function of the arterial lumen sizes (increase in flow resistance in the hydraulic system); 0—no reduction-, 1—first-, 2—second stage of the reduction of the blood vessel lumen.

Decreasing the vessel lumen results in consecutive increases in aortic and left ventricular pressures, while there is no effect on their frequency-dependent values. The effect of frequency is evident between frequencies of 60 and 100 cyc/min. Above 100 cyc/min, the operating frequency has little effect on pressure values.

The results obtained in terms of pressure measurements mean that the innovative implantable LVAD proposed here can operate over a wide frequency range, i.e., from 60 to 160 cyc/min, extending the applicability of the device at much higher operating frequencies than in [35].

Increasing the operating frequency of the device results in a linear increase in energy consumption. Significantly, the effect of reducing the lumen of the vessel has a negligible effect on energy consumption. Another finding is that the part of the power, which was labeled P_1, is constant, regardless of the operating conditions of the device.

The innovative implantable LVAD is able to increase the mass flow rate by approximately 50% in the absence of the reduction of the blood vessel lumen with an increase in operating frequency, from 60 to 160 cyc/min. One of the reasons the device works effectively is that, in addition to supporting the left ventricle, the valve balloon occludes the mitral valve. This is a unique solution, which is unknown in the literature—the essence of which is to simultaneously block the flow through the mitral valve during systole, as well as the ejection of blood from the left ventricle into the aorta at the same time. The solutions known in the literature only support the ventricles without simultaneous valve occlusion, e.g., [16,17,32,36–41].

Another advantage of the proposed LVAD is the minimally invasive method of implantation, which is important for patients with end-stage heart failure. This also means that it complements support in patients previously ineligible or qualified with bad results, i.e., pulmonary hypertension.

5. Conclusions

One of the most important conclusions is that the innovative implantable left ventricle assist device allows operating at high frequencies, up to 160 cyc/min. The study also shows that—above 140 cyc/min—the mass flow rate increment is no longer achieved for specified initial conditions, e.g., an initial gas pressure of 75 mm Hg. The increase in mass flow rate at maximum frequency for the case without reduction of the vessel lumen reaches a maximum of 50% compared to the standard case of 60 cyc/min. Thus, the proposed circulatory assist device is capable of increasing blood ejection into the aorta. This is also possible because the mitral valve is completely occluded by the valve balloon. Additionally, with a higher initial pressure in the pneumatic system, the flow rate would probably be higher. This also applies to the suction–discharge device used, with a crank stroke of 40 mm. Increasing the stroke could further increase the flow rate.

Finally, as far as balloon pressure is concerned, it increases with the frequency of operation, as well as with the reduction of the vessel lumen. The same is true for the aorta

and left ventricle. The greatest pressure changes relative to a frequency of 60 cyc/min are observed between the frequencies of 60 and 100 cyc/min. Further increases in frequency do not result in larger pressure increments. This is correct for all cases of reducing the vessel lumen. The obtained pressures in the ventricle and aorta, owing to the adjustable valve used, correspond very well to the real pressures of the human heart. It follows that the designed test stand allows for a realistic simulation of the circulatory system, which implies that other devices could also be tested on it in the future.

Author Contributions: R.J.: conceptualization; methodology; data curation; visualisation, investigation, validation. K.T.: conceptualization; formal analysis; methodology; supervision; project administration; investigation; writing—original draft. L.D.: conceptualization; methodology; data curation; visualisation, investigation. J.R.: conceptualization; methodology; medical supervision. All authors have read and agreed to the published version of the manuscript.

Funding: This work was supported by the National Centre for Research and Development, Poland, POIR.01.01.01-00-1026/18.

Institutional Review Board Statement: This study was executed in strict accordance with the recommendations for Good Clinical Practice. The protocol was approved by the Independent Bioethics Committee with permission number NNKBN 167/2017.

Informed Consent Statement: Informed consent was obtained from all subjects involved in the study.

Data Availability Statement: The data presented in this study are available upon request from the corresponding author. The data are not publicly available due to privacy.

Conflicts of Interest: All authors were employed by Medarch, Ltd., which carried out grant POIR.01.01.01-00-1026/18. In addition, the authors declare that this research was conducted without any commercial or financial relationships that could be construed as a potential conflict of interest.

References

1. Cardiovascular Diseases. Available online: https://www.who.int/health-topics/cardiovascular-diseases (accessed on 15 October 2023).
2. Lippi, G.; Sanchis-Gomar, F. Global epidemiology and future trends of heart failure. *AME Med. J.* **2020**, *5*, 2520–0518. [CrossRef]
3. Palazzolo, T.; Hirschhorn, M.; Garven, E.; Day, S.; Stevens, R.M.; Rossano, J.; Tchantchaleishvili, V.; Throckmorton, A.L. Technology landscape of pediatric mechanical circulatory support devices: A systematic review 2010–2021. *Artif. Organs* **2022**, *46*, 1475–1490. [CrossRef] [PubMed]
4. Benjamin, E.J.; Blaha, M.J.; Chiuve, S.E.; Cushman, M.; Das, S.R.; Deo, R.; de Ferranti, S.D.; Floyd, J.; Fornage, M.; Gillespie, C.; et al. Heart disease and stroke statistics—2017 update: A report from the American heart association. *Circulation* **2017**, *135*, 146–603. [CrossRef]
5. Li, Y.; Xi, Y.; Wang, H.; Sun, A.; Deng, X.; Chen, Z.; Fan, Y. A new way to evaluate thrombotic risk in failure heart and ventricular assist devices. *Med. Nov. Technol. Devices* **2022**, *16*, 100135. [CrossRef]
6. Maddox, T.M.; Januzzi, J.L., Jr.; Allen, L.A.; Breathett, K.; Butler, J.; Davis, L.L.; Fonarow, G.C.; Ibrahim, N.E.; Lindenfeld, J.; Masoudi, F.A.; et al. 2021 Update to the 2017 ACC expert consensus decision pathway for optimization of heart failure treatment: Answers to 10 pivotal issues about heart failure with reduced ejection fraction: A report of the American College of Cardiology Solution Set Oversight Committee. *J. Am. Coll. Cardiol.* **2021**, *77*, 772–810. [CrossRef] [PubMed]
7. Mancini, D.; Colombo, P.C. Left ventricular assist devices: A rapidly evolving alternative to transplant. *J. Am. Coll. Cardiol.* **2015**, *65*, 2542–2555. [CrossRef]
8. Quader, M.; Toldo, S.; Chen, Q.; Hundley, G.; Kasirajan, V. Heart transplantation from donation after circulatory death donors: Present and future. *J. Card. Surg.* **2020**, *35*, 875–885. [CrossRef]
9. Berk, Z.B.K.; Zhang, J.; Chen, Z.; Tran, D.; Griffith, B.P.; Wu, Z.J. Evaluation of in vitro hemolysis and platelet activation of a newly developed maglev LVAD and two clinically used LVADs with human blood. *Artif. Organs* **2019**, *43*, 870–879. [CrossRef]
10. Heidenreich, P.A.; Albert, N.M.; Allen, L.A.; Bluemke, D.A.; Butler, J.; Fonarow, G.C.; Ikonomidis, J.S.; Khavjou, O.; Konstam, M.A.; Maddox, T.M.; et al. Forecasting the impact of heart failure in the United States. A policy statement from the American heart association. *Circ. Heart Fail.* **2013**, *6*, 606–619. [CrossRef]
11. Roth, G.A.; Mensah, G.A.; Johnson, C.O.; Addolorato, G.; Ammirati, E.; Baddour, L.M.; Barengo, N.C.; Beaton, A.Z.; Benjamin, E.J.; Benziger, C.P.; et al. Global Burden of Cardiovascular Diseases and Risk Factors, 1990–2019: Update from the GBD 2019 Study. *J. Am. Coll. Cardiol.* **2020**, *76*, 2982–3021. [CrossRef]
12. Farrar, D.J.; Hill, J.D.; Gray, L.A., Jr.; Pennington, D.G.; McBride, L.R.; Pierce, W.S.; Pae, W.E.; Glenville, B.; Ross, D.; Galbraith, T.A.; et al. Heterotopic prosthetic ventricles as a bridge to cardiac transplantation. *N. Engl. J. Med.* **1988**, *318*, 333–340. [CrossRef] [PubMed]

13. Hrobowski, T.; Lanfear, D.E. Ventricular assist devices: Is destination therapy a viable alternative in the non-transplant candidate? *Curr. Heart Fail. Rep.* **2013**, *10*, 101–107. [CrossRef] [PubMed]
14. Sawa, Y. Current status of third-generation implantable left ventricular assist devices in Japan, Duraheart and HearWare. *Surg. Today* **2015**, *45*, 672–681. [CrossRef]
15. Tesch, K.; Kaczorowska, K. Arterial cannula shape optimization by means of the rotational firefly algorithm. *Flow Eng. Optim.* **2014**, *48*, 497–518. [CrossRef]
16. Sarna, J.; Kustosz, R.; Major, R.; Lackner, J.M.; Major, B. Polish artificial heart—New coatings, technology, diagnostics. *Bull. Pol. Acad. Sci. Tech. Sci.* **2010**, *58*, 329–335. [CrossRef]
17. Noon, G.P.; Morley, D.; Irwin, S.; Benkowski, R. Development and clinical application of the MicroMed DeBakey VAD. *Curr. Opin. Cardiol.* **2000**, *15*, 167–171. [CrossRef] [PubMed]
18. Abrams, D.; Combes, A.; Brodie, D. Extracorporeal membrane oxygenation in cardiopulmonary disease in adults. *J. Am. Coll. Cardiol.* **2014**, *63*, 2769–2778. [CrossRef] [PubMed]
19. Takayama, H.; Truby, L.; Koekort, M.; Uriel, N.; Colombo, P.; Mancini, D.M.; Jorde, U.P.; Naka, Y. Clinical outcome of mechanical circulatory support for refractory cardiogenic shock in the current era. *J. Heart Lung Transplant.* **2013**, *32*, 106–111. [CrossRef]
20. Sed, D.; Kabir, T.; Lees, N.J.; Stock, U. Valvular complications following the Impella device implantation. *J. Card. Surg.* **2021**, *36*, 1062–1066. [CrossRef]
21. Stewart, G.C.; Givertz, M.M. Mechanical circulatory support for advanced heart failure: Patients and technology in evolution. *Circulation* **2012**, *125*, 1304–1315. [CrossRef] [PubMed]
22. Teuteberg, J.J.; Cleveland, J.C., Jr.; Cowger, J.; Higgins, R.S.; Goldstein, D.J.; Keebler, M.; Kirklin, J.K.; Myers, S.L.; Salerno, C.T.; Stehlik, J.; et al. The Society of Thoracic Surgeons Intermacs 2019 annual report: The changing landscape of devices and indications. *Ann. Thorac. Surg.* **2020**, *109*, 649–660. [CrossRef] [PubMed]
23. Kirklin, J.K.; Naftel, D.C.; Pagani, F.D.; Kormos, R.L.; Stevenson, L.W.; Blume, E.D.; Miller, M.A.; Baldwin, J.T.; Young, J.B. Sixth INTERMACS annual report: A 10,000-patient database. *J. Heart Lung Transplant.* **2014**, *33*, 555–564. [CrossRef] [PubMed]
24. Walther, C.P.; Niu, J.; Winkelmayer, W.C.; Cheema, F.H.; Nair, A.P.; Morgan, J.A.; Fedson, S.E.; Deswal, A.; Navaneethan, S.D. Implantable ventricular assist device use and outcomes in people with end-stage renal disease. *J. Am. Heart Assoc.* **2018**, *7*, e008664. [CrossRef] [PubMed]
25. Pleșoianu, F.A.; Pleșoianu, C.E.; Bararu Bojan, I.; Bojan, A.; Țăruș, A; Tinică, G. Concept, design, and early prototyping of a low-cost, minimally invasive, fully implantable left ventricular assist device. *Bioengineering* **2022**, *9*, 201. [CrossRef] [PubMed]
26. Shah, S.P.; Mehra, M.R. Durable left ventricular assist device therapy in advanced heart failure: Patient selection and clinical outcomes. *Indian Heart J.* **2016**, *68*, S45–S51. [CrossRef]
27. Aaronson, K.D.; Slaughter, M.S.; Miller, L.W.; McGee, E.C.; Cotts, W.G.; Acker, M.A.; Jessup, M.L.; Gregoric, I.D.; Loyalka, P.; Frazier, O.H.; et al. Use of an intrapericardial, continuous-flow, centrifugal pump in patients awaiting heart transplantation. *Circulation* **2012**, *125*, 3191–3200. [CrossRef] [PubMed]
28. Rogers, J.G.; Pagani, F.D.; Tatooles, A.J.; Bhat, G.; Slaughter, M.S.; Birks, E.J.; Boyce, S.W.; Najjar, S.S.; Jeevanandam, V.; Anderson, A.S.; et al. Intrapericardial left ventricular assist device for advanced heart failure. *N. Engl. J. Med.* **2017**, *376*, 451–460. [CrossRef]
29. Tesch, K.; Kaczorowska, K. The discrete-continuous, global optimisation of an axial flow blood pump. *Flow Turbul. Combust.* **2019**, *104*, 777–793. [CrossRef]
30. Shi, J.; Yu, X.; Liu, Z. A review of new-onset ventricular arrhythmia after left ventricular assist device implantation. *Cardiology* **2022**, *147*, 315–327. [CrossRef]
31. Bierewirtz, T.; Narayanaswamy, K.; Giuffrida, R.; Rese, T.; Bortis, D.; Zimpfer, D.; Kolar, J.; Kertzscher, U.; Granegger, M. A Novel Pumping Principle for a Total Artificial Heart. *IEEE Trans. Biomed. Eng.* **2023**, 1–10. [CrossRef]
32. Goodin, M.S.; Horvath, D.J.; Kuban, B.D.; Polakowski, A.R.; Fukamachi, K.; Flick, C.R.; Karimov, J.H. Computational fluid dynamics model of continuous-flow total artificial heart: Right pump impeller design changes to improve biocompatibility. *ASAIO J.* **2022**, *68*, 829–838. [CrossRef] [PubMed]
33. Tesch, K.; Jasinski, R.; Dabrowski, L.; Rogowski, J. Experimental investigation of the performance of an innovative implantable left ventricular assist device—Proof of concept. *Appl. Sci.* **2023**, *13*, 973. [CrossRef]
34. PCT Application, Implantable Left Ventricular Assist Device and System for Ventricular-Assist for Use in Patients with End-Stage Heart Failure PCT/PL2021/050004. Available online: https://patentscope.wipo.int/search/en/detail.jsf?docId=WO2021162564 (accessed on 11 October 2023).
35. Jasinski, R.; Tesch, K.; Dabrowski, L.; Rogowski, J. Innovative Implantable Left Ventricular Assist Device—Performance under Various Resistances and Operating Frequency Conditions. *Appl. Sci.* **2023**, *13*, 7785. [CrossRef]
36. Impella® The World's Smallest Heart Pump. Available online: https://www.abiomed.com/products-and-services/impella(accessed on 15 October 2023).
37. John, R.; Liao, K.; Lietz, K.; Kamdar, F.; Colvin-Adams, M.; Boyle, A.; Miller, L.; Joyce, L. Experience with the Levitronix CentriMag circulatory support system as a bridge to decision in patients with refractory acute cardiogenic shock and multisystem organ failure. *Cardiopulm. Support Physiol.* **2007**, *134*, 351–358. [CrossRef]
38. Tempelhof, M.W.; Klein, L.; Cotts, W.G.; Benzuly, K.H.; Davidson, C.J.; Meyers, S.N.; McCarthy, P.M.; Malaisrie, C.S.; McGee, E.C.; Beohar, N. Clinical experience and patient outcomes associated with the TandemHeart percutaneous transseptal assist device among a heterogeneous patient population. *ASAIO J.* **2011**, *57*, 254–261. [CrossRef]

39. Schmitto, J.D.; Pya, Y.; Zimpfer, D.; Krabatsch, T.; Garbade, J.; Rao, V.; Morshuis, M.; Beyersdorf, F.; Marasco, S.; Sood, P.; et al. Long-term evaluation of a fully magnetically levitated circulatory support device for advanced heart failure—Two-year results from the HeartMate 3 CE Mark Study, *Eur. J. Heart Fail.* **2019**, *21*, 90–97. [CrossRef]
40. Available online: https://global.medtronic.com/ (accessed on 15 October 2023).
41. Dykes, J.C.; Bleiweis, M.S.; Maeda, K.; Chen, S.; Rosenthal, D.N.; Tjossem, C.; Murray, J.; Almond, C.S. Berlin Heart outcomes in single ventricle patients: where are we now? *J. Heart Lung Transplant.* **2018**, *37*, S102. [CrossRef]